Chem. Res. Chin. Univ., 2016, 32(4), 549—555 doi: 10.1007/s40242-016-6054-1

Electromagnetic Properties of a New Microwave Plasma Torch with Double Resonance Configuration

YU Bingwen[1,2], JIN Wei[1,2*], ZHU Dan[1,2], YING Yangwei[1,2], YU Haixiang[1,2], SHAN Jin[1,2], XU Chen[2], LIU Wenlong[2] and JIN Qinhan[1*]

1. Research Center for Analytical Instrumentation, Institute of Cyber-systems and Control, College of Control Science and Engineering, Zhejiang University, Hangzhou 310058, P. R. China;

2. Zhejiang Supcon Research Co., Ltd., Hangzhou 310058, P. R. China

Abstract In order to obtain a stable plasma and improve the performance of the torch for atomic emission spectroscopy(AES), the structure of microwave plasma torch(MPT) was analyzed. The transmission and distribution characteristics of the electromagnetic field of the torch configuration with two or three concentric tubes, as well as the metal spacer between inner and intermediate tubes with different depths were simulated with electromagnetic simulation software and verified by experiments. The results indicate that the inner tube of MPT plays an important role in strengthening the electric field intensity at the opening end of the MPT and redistributing the electromagnetic field in the whole torch by forming a double resonance configuration, and contributes to enhancing the macroscopic stability and the self-sustainment of the plasma. The stability of the plasma is proved to be excellent when the metal spacer between the inner and intermediate tubes is located at a place 20—30 mm away from the top opening of the torch. A proper location of the spacer can also avoid the formation of a static filament plasma or a rotating plasma rooted from the outer wall of the inner tube. With the help of morphological analysis, the underlying reason why MPT possesses a great tolerance to wet aerosols and air introduction was clearly made, that is, the formation region of the plasma formed with MPT is apparently separated from the reaction zone of it.

Keywords Microwave plasma torch(MPT); Double resonance configuration; Electromagnetic simulation

1 Introduction

The microwave plasma torch(MPT) was first developed as a new excitation source of atomic emission spectrometry(AES) by Jin *et al*.[1] in 1985. The structure of MPT is similar to that of ICP torch with triple coaxial tubes. However, MPT can not only be operated with argon, but also with helium, nitrogen or even air at atmospheric pressure with low microwave forward power. The plasma formed with MPT presents an inverted funnel shape, which is beneficial to the introduction of samples, and is highly tolerant to the introduction of wet aerosols and molecular species[2,3]. Up to now, as an emission source for AES, excellent characteristics of MPT have won numerous domestic and foreign peer recognition. More than 270 papers have been published by authors from 20 plus laboratories around the world. A monograph entitled "Microwave Induced Plasma Analytical Spectrometry" was published by the Royal Society of Chemistry Publishing(UK) in 2011, which summarized 15 milestones in the development history of microwave plasma spectrometry since 1950, the achievements of MPT occupied three of them[4].

Since the development of MPT, quite a few scholars have made lots of improvements in many aspects, including the geometry and material, the means of microwave coupling (conductively or capacitively coupled), the coupling position, the means of tuning, and keeping concentricity, the introduction of shielding gas and/or shielding case as well as gas resistance configuration, in order to improve the excitation power and analytical performance[2,5—10]. Essentially, all these methods used to optimize the distribution of electromagnetic field and flow field are empirical(trial and error methods). However, it is a pity that so far rarely did scholars make a systematic and specific theoretical analysis on the resonant structure of electromagnetic field in MPT. The lack of theoretical knowledge has brought difficulties to the development of kilowatt MPT(kW-MPT) technology[11]. In fact, during the course of experimental study, with the increase of microwave forward power, a valuable and stable inverted funnel shaped plasma is hard to be formed and a standing single filament plasma tends to be formed, which is useless for analytical application.

In view of the above mentioned reasons, the structure of MPT was analyzed by means of simulation of the electromagnetic field in this work. The effect of each part of the torch on transmission and distribution of the electromagnetic field was

*Corresponding authors. E-mail: jinweimy@zju.edu.cn; qhjin@zju.edu.cn

Received February 17, 2016; accepted April 28, 2016.

Supported by the National Key Scientific Instrument and Equipment Development Project of China(No.2013YQ470781).

discussed and accompanied with verification of experiments. Based on such deep theoretical cognition, a novel MPT with double resonance configuration was developed, and a quite stable plasma was sustainable with it at a higher microwave forward power up to kilowatts with argon or helium as supporting gas at atmospheric pressure.

2 Structure of MPT and Early Knowledge

Fig.1 shows the basic structure of an MPT, which is constituted with three coaxial tubes. The outer tube is made from brass, the intermediate tube prefers copper with excellent electrical conductivity, and the inner tube can be made from copper or quartz. During the operation, the microwave energy is transmitted into the resonant cavity with an opening end in transverse electromagnetic mode(TEM) *via* a coaxial cable with 50 or 75 Ω resistance. Once the depth of the cavity(the distance between the opening end and the short-circuited end) satisfies the certain conditions, a stable standing wave field will be formed in the cavity. In order to get the strongest electrical field and the weakest magnetic field at the opening end, the cavity depth is generally designed to be the odd-multiple of 1/4 wavelength of the microwave radiation used. The support and carrier gases are introduced through the intermediate and inner tubes, respectively. With the interaction of microwave energy and the plasma support gas at the opening end, the plasma gas is breakdown and then the plasma is sustained.

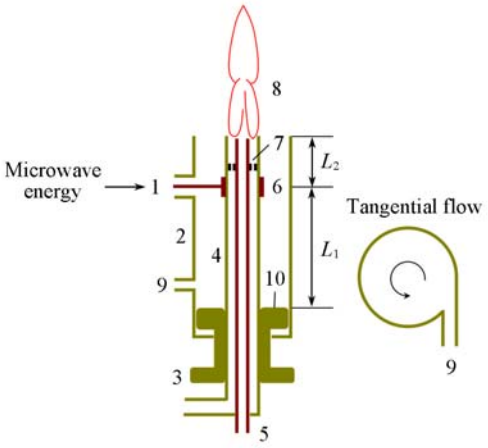

Fig.1 Schematic diagram of MPT

1. Microwave inlet; 2. outer tube; 3. tuning stub; 4. intermediate tube; 5. inner tube; 6. coupling loop; 7. spacer; 8. plasma flame; 9. shielding gas inlet; 10. short-circuited end.

Fig.2 shows the electric and magnetic fields of the MPT with (3/4)λ cavity depth. Wang[12] and Yang[13] believed that the greatest density of the electric-field lines was located at a certain distance from the opening end(usually 6—12 mm). This was because of the bending of electric-field lines and the electric fields being superimposed there, and it also indicated why there was a brightest "intersection" region in the plasma sustained by MPT, as well as a central channel, which was beneficial for the introduction of sample and the better interaction between analytes and plasma. Bilgic *et al.*[8,14] made a simulation of MPT structure by a finite difference time domain(FDTD) method, and the results showed that the maximum electric field strength of MPT was located at the outside corner of the intermediate tube and extended to the central channel, where the plasma was mainly generated. The axial symmetric distribution of the peak electric field strength was also confirmed by the hollow structure of the plasma. But it was difficult to make a clear explanation for the formation of the inverted funnel shaped plasma obtained from MPT, whose root was located between the intermediate tube and the inner tube. Besides, they took only a part structure of the outer tube and the intermediate tube into consideration, while ignoring the influence of the inner tube on the electromagnetic field distribution. After further detailed analysis of MPT, it was found that not only the outer tube and intermediate tube constituted a main coaxial section, but also the intermediate tube and inner tube constituted a secondary coaxial section. Furthermore, the distance between the opening end and the metal spacer with holes(part 7 in Fig.1), which is used to guarantee the concentricity of the intermediate tube and the inner tube in the practical work, does have an important influence on the electromagnetic distribution between the intermediate and the inner tube, and it is exactly a significant factor that the predecessors ignored when studying the structure of the MPT.

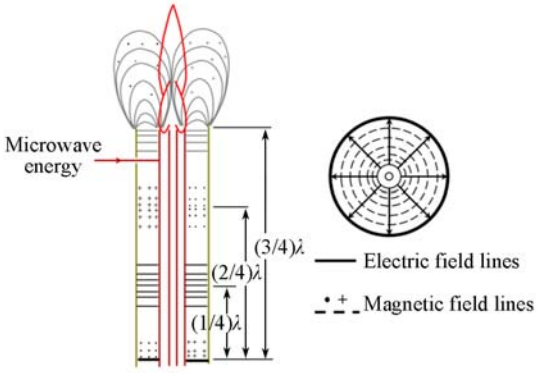

Fig.2 Electric and magnetic fields of MPT

3 Simulation Part

3.1 Model Establishment

Based on the above-mentioned analysis, the transmission and distribution of electromagnetic field in MPT cavity were simulated using multi-physics software COMSOL multiphysics in this paper. In order to explore the role played by every part of MPT in the transmission and distribution of electromagnetic fields, the simulation model was based on the simplest structure of two coaxial tubes first, and gradually approached its actual structure. The difference between this work and the work done by Bilgic *et al.*[8,14] was that the influence of the microwave coupling loop on the whole model was taken into account here to regard the simulation domain as a non-axial symmetry. The total three-dimensional model of MPT is shown in Fig.3. Besides, it is difficult to obtain the spatial distribution of the electron density of MPT plasma due to the limitation of experimental conditions and the equivalent medium model of the plasma is hardly established, so in this study, only the characteristics of an MPT cold cavity are considered.

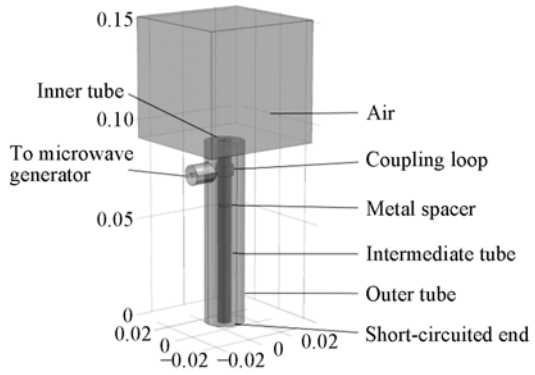

Fig.3 Schematic diagram of 3D simulation model of MPT(unit: m)

The related dimensions and materials of the MPT in the simulation model are listed in Table 1 and Table 2 unless otherwise stated. Considering that the electrical characteristics of argon, oxygen and air are very close, air was chosen as the gas material used in this simulation. The microwave frequency was 2450 MHz and microwave generator power was set at 100 W.

Table 1 Dimensions of the MPT in this simulation model(mm)*

L_1	L_2	D	d	d_i	d_{ao}	d_{ai}
78.3	13.5	20	7	6	3	2

* D is the inner diameter of the outer tube; d is the outer diameter of the intermediate tube; d_i is the inner diameter of the intermediate tube; d_{ao} is the outer diameter of the inner tube and d_{ai} is the inner diameter of the inner tube.

Table 2 Material properties used in the simulation model

Material	Relative permittivity	Relative permeability	Electrical conductivity/(S·m^{-1})
PTFE*	2	1	10^{-25}—10^{-23}, choose 0
Copper	1	1	5.998×10^{7}
Air	1	1	0

* PTFE: Polytetrafluoroethylene.

3.2 Discussion of Simulation Results

3.2.1 MPT with Two Coaxial Tubes

The electric field distribution of MPT with two coaxial tubes is shown in Fig.4. It is noteworthy that all the figures shown in this manuscript are the cross sections of the 3D images for a better visual display. It can be seen from Fig.4(A) that a standing-wave electric field profile is formed in the main coaxial section, and the local maximum electric field strength of MPT is located at the odd-multiple of 1/4 wavelength away from the short-circuited end. The distribution of the electric field norm extracted along the inner wall and the outer wall of the intermediate tube is shown in Fig.4(B). Due to the presence of the coupling loop, the data are interrupted and cut into two parts. It can be seen that the peak electric field strength(about 316.5 kV/m) is located at the outer corner of the intermediate tube as a result of the electromagnetic standing-wave distribution and the fringe field effect, which is sufficient to ionize plasma gas, such as argon, to form a plasma. However, the electric field energy in the main coaxial section has not been transmitted to the interior of the intermediate tube, and the electric field strength decreases exponentially with depth in a range of about 3 mm away from the opening end of the tube, which is consistent with the conclusion in the relevant references[8,14].

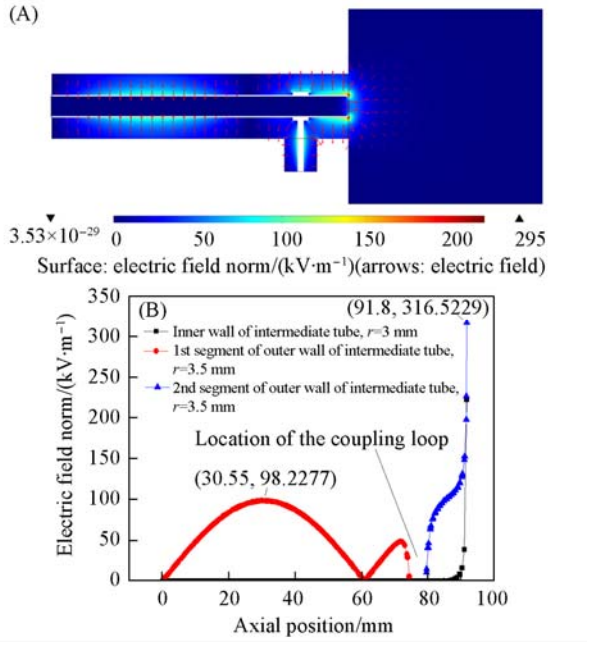

Fig.4 Electric field norm distributions of torch with two coaxial tubes(A) and along the inner wall and outer wall of the intermediate tube(B)

The horizontal axis refers to the distance from the short-circuited end, and the character '*r*' in the legend refers to the radius of the data extracted, the same below.

3.2.2 MPT with Three Coaxial Tubes

When the inner tube was added to the torch model, the electromagnetic field will redistribute as shown in Fig.5. The difference of the configuration between MPT with three coaxial tubes and that with two coaxial tubes is that the electromagnetic field in the main coaxial section can be transmitted into the section between the intermediate tube and the inner tube (the secondary coaxial section) through the opening end of the torch in TEM mode. The electric field there exhibits the same standing wave pattern except the electric field strengths as that in the main coaxial section when the depths of the two sections are equal. However, the electromagnetic field cannot be further transmitted into the inner tube. Taking into account that the inner tube can be regarded as a circular(hollow metal pipe) waveguide, and the cross section of circular waveguide is a single conductor, therefore, the TEM waves cannot propagate in the inner tube according to the electromagnetic theory. In addition, it can be seen from the circular waveguide propagation mode that for a circular waveguide, the electromagnetic waves cannot propagate anymore when operating wavelength λ is greater than 3.41 times the radius of the circular waveguide. In other words, it cannot propagate any TE/TM electromagnetic wave apart from TEM wave. The inner diameter of the MPT inner tube is r=2 mm and $3.41r$ <<122.4 mm, so the inner tube plays a role of cutoff waveguide here. As shown in Fig.5(B), in the same horizontal cross-section(*i.e.*, the identical axial position), the standing wave electric field strength in the secondary

coaxial section is stronger than that in the main coaxial section, which means that the characteristics and the role of the electromagnetic field in the secondary coaxial section cannot be ignored in practical research. Furthermore, the peak electric field strength is still located at the outer corner of the intermediate tube regardless of the presence of the secondary coaxial section.

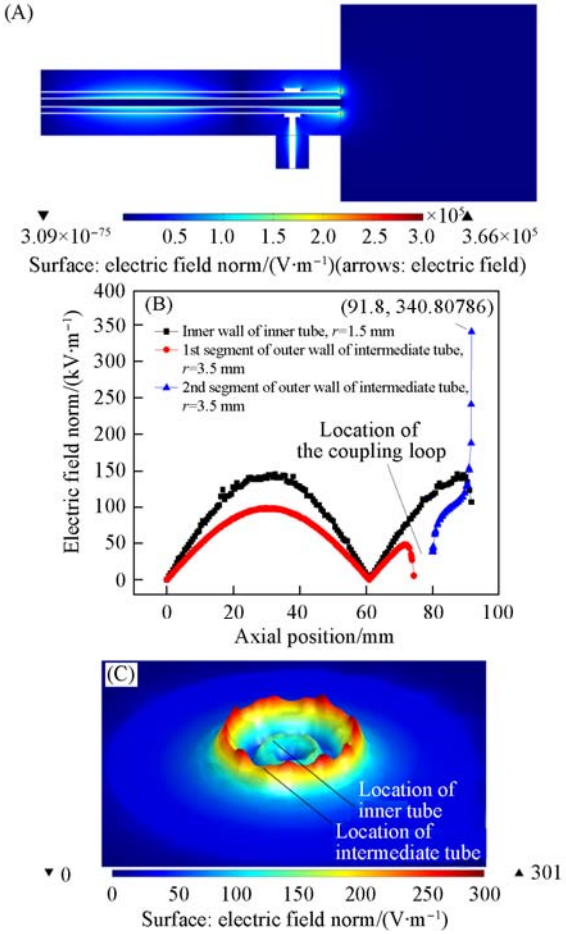

Fig.5 Electric field norm distributions of torch with three tubes(A), along the outer wall of intermediate tube and inner tube of MPT(B) and at the opening end of MPT(C)

Fig.5(C) illustrates the electric field norm distribution at the opening end of MPT. It can be seen clearly that the electric field is axial symmetric distributed and the peaks of the electric field strength are located at the opening end of each tube, which meets completely the requirements of an ideal plasma excitation source for an radial electric field distribution[15]. The electric field strength is relatively weak in the inner tube at the opening end, and the characteristics of the central channel of the plasma formed can be well deduced from the distribution of electric field as discussed above. The radial electric field strengths at different depths within the cavity of MPT show a similar axisymmetric distribution to Fig.5(C).

3.2.3 MPT with Double Resonance Configuration

Since the configuration of resonant cavity with an opening end can also be formed in the secondary coaxial section, the depth of the cavity becomes a significant factor influencing the distribution of electromagnetic field. Furthermore, the characteristic of the double resonance configuration of MPT can be obtained when both of the main and the secondary coaxial section meet the conditions of forming a stable standing wave field. Initially, the design of intermediate tube and inner tube is limited by the tuning range and the size of tuning window, so that the lengths of the two tubes are not the same. Besides, in the development of MPT-AES, nonmetal materials, such as PTFE, ceramics, etc. have been used as a spacer to ensure the concentricity of intermediate tube and inner tube by some scholars[5], while others chose a metal one[2]. The former materials are transparent to microwave, so the effective depth of the secondary coaxial section of cavity is basically the same as its actual depth, but the latter one(metal spacer) can reflect microwave, so the effective depth of the secondary coaxial section of the cavity is limited to the distance between the opening end and the spacer. In conclusion, the effective depth of the cavity in the secondary coaxial section is the key factor of MPT with double resonance configuration.

A simulation in respect to different cavity depth in the secondary coaxial section under the former conditions(take PTFE material as an example) was carried out first in this section. Considering the periodic characteristic of the standing wave, the range of simulated cavity depth is set in 92—124 mm, which spans about $\lambda/4$, and the electric distributions along the outer wall of intermediate tube and inner tube are shown in Fig.6(A) and (B), respectively. The simulation results show that the change of the secondary coaxial section depth does not influence the electric distribution in the main coaxial section, and the typical electric field norm distribution is shown in Fig.6(A). However, the electric field distribution in the secondary coaxial section, especially the amplitude of the electric field, varies a lot under different conditions. Generally speaking, when the depth of the cavity approaches to an odd multiple of $\lambda/4$(*e.g.*, 92 mm), the electric field strength reaches a maximun.

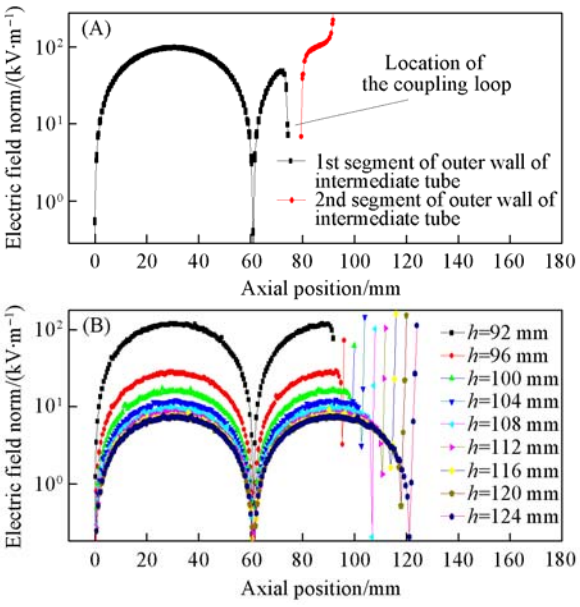

Fig.6 Electric field norm distributions along the outer wall of intermediate tube(A) and the inner tube(B) at different cavity depths in the secondary coaxial section

On the contrary, when the depth of the cavity is close to an even number times of $\lambda/4$(*e.g.*, 124 mm), the microwave energy transmitted into the secondary coaxial section is relatively low and, therefore, the electric field strength there is weak. This phenomenon indicates that the tuning characteristics of the main coaxial section and the secondary coaxial section are similar, as shown in Fig.6(B), where the location of the short-circuited end in the secondary coaxial section is set as the coordinate origin.

Fig.7 and Fig.8 illustrate how the electric field norm distribution changes along with the depths of the metal spacer. It can be noted that the scales of the legend used in the subgraphs of Fig.7 are different. According to the simulation results, the electromagnetic wave almost does not propagate into the region between the intermediate and the inner tubes unless the metal spacer is located at the place close to $\lambda/4$ away from the opening end. As shown in Fig.7 and Fig.8, when the depth of the metal spacer is set at 30 mm from the opening end, a maximum electric field norm of 2204 kV/m is reached, and the electric field strength in the secondary coaxial section is much higher than that in the main coaxial section at the same cross section.

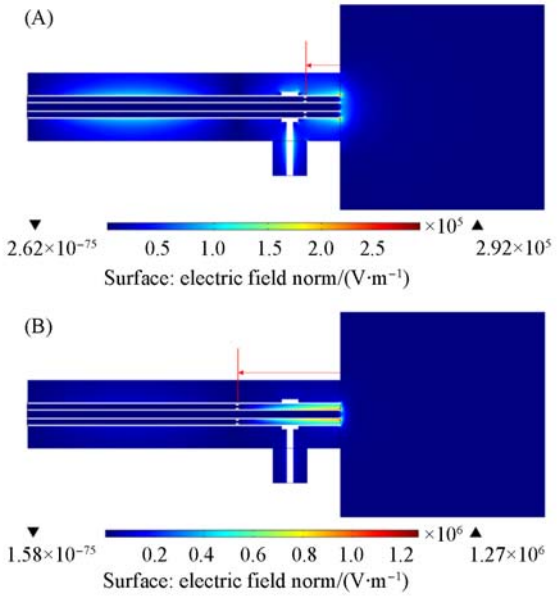

Fig.7 Electric field norm distributions of MPT with the depths of metal spacer being 10(A) and 30 mm(B), respectively

The red arrow indicates the depth of the metal spacer.

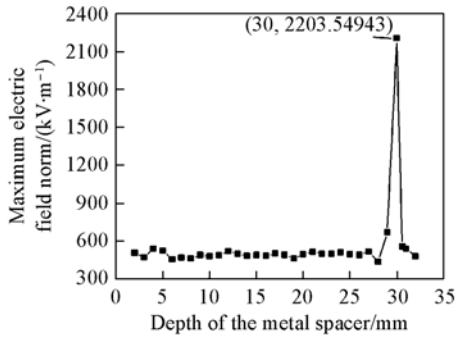

Fig.8 Maximum electric field norm changing with the depths of the metal spacer

The maximum value was extracted from the entire computational domain of the model; microwave power: 100 W.

4 Experimental

Since the intermediate tube and the inner tube are located inside the MPT, it is difficult to construct an experiment for the measurement of the electromagnetic field distribution at the secondary coaxial section, which emphasizes on the apparent effect of the inner tube and the depth of the metal spacer on the shape of the MPT plasma.

An FYC-013-type solid state microwave generator manufactured by Nanjing Fengyan Corporation(Nanjing, China) was used in the experiment to provide microwave energy(the frequency: 2450 MHz; the range of power: 0—100 W). The support gas and carrier gas used in the experiment were both argon with a purity of 99.999%, the shielding gas was oxygen with a purity of 99.999%. The structure and dimensions of the torch were the same as those aforementioned and all the photographs of MPT below were taken by a digital camera of NIKON D7000 type.

4.1 Effect of Inner Tube

In this experiment, the inner tube was removed while other parameters remained unchanged. That was, the microwave forward power was set at 100 W, the flow-rate of the support gas was 0.9 L/min, and the flow-rate of shielding gas was 1.5 L/min. The plasma was ignited and some typical photos of the plasma was taken with the camera. Unless otherwise stated, the *f*-number of the camera was set to be F5.6 while the exposing time was 1/50 s.

The results reveal that for a torch with only an outer tube and an intermediate tube, there are two different types of morphology of the plasma: (1) single static plasma filament locating fixedly at a certain position on the inner wall of the intermediate tube; (2) single filament discharge rotating slowly along the inner wall of the intermediate tube close to its opening end.

Fig.9 illustrates that the single filament Ar-MPT plasma formed with two-tube torch(without the inner tube) rotates along the inner wall of the intermediate tube. The rotational

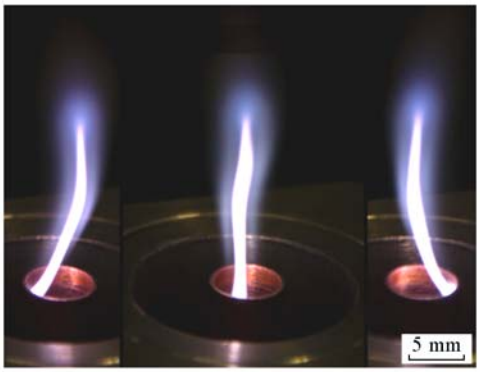

Fig.9 Photographs of oxygen-shielded Ar-MPT (OS-ArMPT) with two tubes

Three typical snapshots for the spatial position of the plasma filament when the plasma filament rotated slowly. Exposure time: 1/200 s, microwave power: 100 W.

speed of the plasma is relatively slow, the camera cannot catch the stable plasma within 1/50 s. And the exposure time was set at 1/200 s in order to record the plasma behavior instantaneously. Here, three typical snapshots for the spatial position of the plasma filament are chosen for analysis.

For the configuration of MPT constituted of two tubes (Fig.9), the root of the plasma filament does not locate at the opening end of the intermediate tube but moves a bit down along its inner wall. This phenomenon appeared also for the routine MPT with three tubes. In combination with the simulation result in Fig.4, it can be concluded that the electromagnetic distribution also exists in the inner wall of the intermediate tube along a certain depth away from the opening end, and the electromagnetic energy transmitted to this local region can sustain plasma after its successful ignition. In addition, when the inner tube is removed, the support gas and the carrier gas mix together, so that the flow field is completely changed, which will finally influence the shape of the plasma. Since the rotational speed of plasma filament is slow, rotational acoustic noise can be clearly heard during the experiment, and meanwhile, the sample analyzed coming out from the intermediate tube cannot completely interact with the plasma, so the optical detection system cannot catch a stable spectrum signal. Obviously, all the above-mentioned factors are disadvantageous for spectral analysis because they will influence seriously the stability and excitation capability of the source.

4.2 Verification of MPT with Double Resonance Configuration

Placed the metal spacer with small holes in the region between the inner tube and the intermediate tube at the positions of 10, 15, 20, 25 and 30 mm away from the top opening end, respectively, and set the flow-rates of support gas and carrier gas both to be 0.6 L/min and the shielding gas to be 0.4 L/min, the microwave forward power remained unchanged. Then we ignited the plasma and recorded the apparent shape of the plasma under different conditions.

Fig.10 illustrates two typical snapshots of plasma morphology when the metal spacer was placed at different depths.

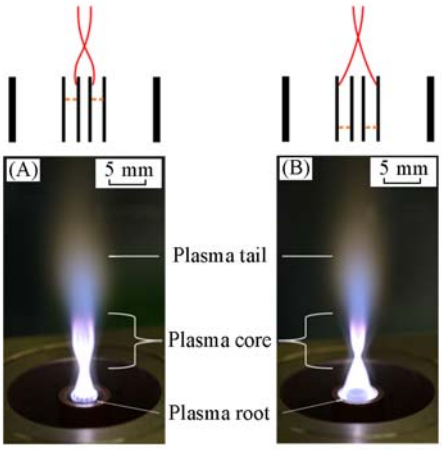

Fig.10 Influence of different depths of the metal spacer on the plasma morphology

Microwave power: 100 W. (A) h=15 mm; (B) h=25 mm.

The results indicate that when the depth of the metal spacer is less than 15 mm, the plasma tends to perform as shown in Fig.10(A) or to be a static single plasma filament. On the contrary, when the depth of metal spacer is in the range of 20—30 mm, the plasma tends to perform as shown in Fig.10(B), which is a normal state.

The two types of plasma shown in Fig.10 were both formed by a single filament discharge on the microscopic time scale[16,17] because of the skin effect[11]. Since a partial region of this kind of filament plasma located near the axis steadily, a temporally and spatially stable region was formed along with the high speed rotational motion of the plasma filament, which finally led to the formation of an inverted funnel-shaped plasma with a “central channel”. In addition, the torch would not be heated significantly by the plasma due to its high rotational speed[18](the rotational frequency of ArMPT is typically 100 Hz). The heat generated would also be taken away from the wall surface through the convection by high gas flow-rate, explaining why the emission spectra taken from MPT plasma suffered no contamination from emission spectral lines of the torch material, *i.e.*, copper lines.

For the first type of plasma morphology[Fig.10(A)], the root of the plasma locates mainly at the outer wall of inner tube, and part of the plasma filament can also form on the inner wall of the inner tube away from the opening end, which is bad to spectral analysis. Since the inner tube is mainly used for sample introduction, sample aerosol would interact directly with the root of the plasma after coming out from the inner tube or even in the inner tube, which can damage the continuity of the energy transmission, weaken the stability of the plasma and reduce the tolerance capacity to sample aerosols. Furthermore, the excitation characteristics of the plasma will be influenced a lot by sample types and characteristics. However, for the second type of plasma morphology[Fig.10(B)], since the root is located between the intermediate tube and the inner tube, away from the opening end, sample aerosol would not interact directly with the plasma root but would interact in the temporally and spatially stable region. This is also one of the reasons why the MPT plasma has a great tolerance to the introduction of wet aerosols and molecular species. Because of the impedance characteristic of the plasma, which is similar to that of a metallic material, and the single filament structure of plasma on the microscopic time scale, while the inner tube is made of metallic material, the presence of the plasma has a limited effect on the electromagnetic field distribution in MPT. Therefore, in practice, the operating range of the depth of the metal spacer is wider than that of the simulation result obtained based on the cold cavity, while the results measured are still basically consistent with that of the simulation.

When the inner tube is made of nonmetal materials, such as quartz, the electromagnetic field distribution of three-tube structure is similar to that of two-tube structure since such nonmetal materials are microwave-transparent materials. However, the local permittivity can be changed due to the presence of the plasma, leading to the change of microwave propagation mode and making it possible to transmit microwave energy into the certain depth in the secondary coaxial

section, which is called local surface wave. The detailed operating mechanism is similar to that of the Surfatron device[19,20]. While in this case, the transmission depth was limited by the presence of short-circuited end and the spacer. Besides, combing with the influence of flow field, the phenomenon that MPT could work with a quartz inner tube can be explained, which is beyond the scope of this paper.

In order to verify the effect of the new MPT with double resonance configuration intuitively, the photographs of 1 kW OS-HeMPT and OS-ArMPT are shown in Fig.11. It can be seen that this new structure can work well under high microwave forward power. It can not only form a stable plasma with argon, or helium, but also inherit the characteristics of plasma under lower microwave forward power(<100 W) with an inverted funnel shape and a central channel, which are beneficial for the sample introduction. In addition, the plasma formed under high operating power conditions has a higher tolerance capacity to wet aerosols and molecular species compared with that formed under the low power conditions. It is a qualitative leap that the sample solution could be directly nebulized into the plasma without the help of desolvation system in the case of OS-ArMPT. And since the helium plasma can be used to determine almost all elements existing in the nature, no matter they are common elements, rare elements, or even nonmetals, kW-MPT-AES could be a brand new valuable technology in the field of atomic emission spectrometry.

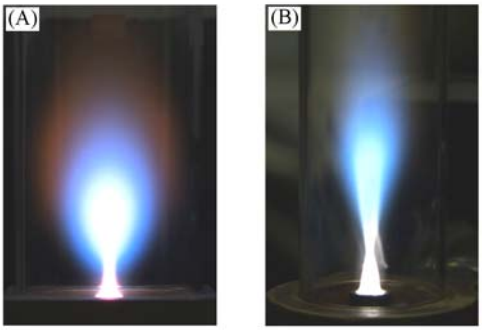

Fig.11 Photos of 1 kW OS-HeMPT(A) and OS-ArMPT(B)

The microwave generator used here was MPG-201C type based on magnetron technology(Chengdu Hueray Microwave Tech. Ltd., China).

5 Conclusions

The electromagnetic field distribution characteristics of MPT cold cavity were theoretically simulated in this paper. The effect of inner tube and metal spacer on the electromagnetic distribution in the torch was discussed in depth and verified with experiments. This research deepens the understanding of functions of each structural component of MPT. Based on that, the structure of MPT was improved and a novel microwave plasma torch with double resonance configuration was developed. A quite stable plasma could be sustained not only under a relatively low microwave forward power, but also under a kilowatt microwave forward power. The results lay down a sound theoretical and technological foundation for the development of high-performance kW-MPT atomic spectrometry.

References

[1] Jin Q., Yang G., Yu A., Liu J., Zhang H., Bi Y., *Acta Scientiarum Naturalium Universitatis Jilinensis*, **1985**, *1*(1), 90

[2] Jin Q., Zhu C., Border M. W., Hieftje G. M., *Spectrochimica Acta Part B: Atomic Spectroscopy*, **1991**, *46*(3), 417

[3] Pereiro R., Wu M., Broekaert J. A. C., Hieftje G. M., *Spectrochimica Acta Part B: Atomic Spectroscopy*, **1994**, *49*(1), 59

[4] Jankowski K. J., Reszke E., *Microwave Induced Plasma Analytical Spectrometry*, Royal Society of Chemistry, London, **2010**

[5] Liu J., Duan Y., Hou M., Li Y., Jin Q., *Analytical Instrumentation*, **1993**, (2), 22

[6] Duan Y., Du X., Li Y., Jin Q., *Applied Spectroscopy*, **1995**, *49*(8), 1079

[7] Yuan X., Zhang H., Cui Z., Ti Z., Jin Q., *Journal of Instrumental Analysis*, **1997**, (4), 3

[8] Bilgic A. M., Prokisch C., Broekaert J. A. C., Voges E., *Spectrochimica Acta Part B: Atomic Spectroscopy*, **1998**, *53*(5), 773

[9] Duan Y., Su Y., Jin Z., Abeln S. P., *Anal. Chem.*, **2000**, *72*(7), 1672

[10] Prokisch C., Broekaert J., *Spectrochimica Acta Part B: Atomic Spectroscopy*, **1998**, *53*(6), 1109

[11] Jin W., Yu B., Zhu D., Ying Y., Yu H., Jin Q., *Chem. J. Chinese Universities*, **2015**, *36*(11), 2157

[12] Wang S., *Studies on the Diagnoses and Application of Oxygen-shielded Argon Microwave Plasma Torch(OS-ArMPT) Excitation Source*, Jilin University, Changchun, **2006**

[13] Yang W., *New Techniques for And Novel Instruments of Microwave Plasma Torch Atomic Emission Spectrometry*, Jilin University, Changchun, **1997**

[14] Bilgic A. M., Garloff K., Voges E., *Plasma Sources Science and Technology*, **1999**, *8*(2), 325

[15] Jankowski K., Reszke E., *J. Anal. Atomic Spectrometry*, **2013**, *28*(8), 1196

[16] van der Mullen J. J. A. M., van de Sande M. J., de Vries N., Broks B., Iordanova E., Gamero A., Torres J., Sola A., *Spectrochimica Acta Part B: Atomic Spectroscopy*, **2007**, *62*(10), 1135

[17] Wang C., Srivastava N., Scherrer S., Jang P., Dibble T. S., Duan Y., *Plasma Sources Science and Technology*, **2009**, *18*(2), 25030

[18] Yu B., Jin W., Ying Y., Yu H., Zhu D., Shan J., Liu W., Xu C., Jin Q., *J. Anal. Atomic Spectrometry*, **2016**, *31*(3), 759

[19] Selby M., Hieftje G. M., *Spectrochimica Acta Part B: Atomic Spectroscopy*, **1987**, *42*(1/2), 285

[20] Moisan M., Beaudry C., Leprince P., *Plasma Science, IEEE Transactions on*, **1975**, *3*(2), 55